High-sensitivity vision restoration via ectopic expression of chimeric rhodopsin in mice

Yusaku Katada[1,2], Kazuho Yoshida[3], Kenta Kobayashi[4], Hideyuki Okano[5], Hideki Kandori[3], Kazuo Tsubota[2*], Toshihide Kurihara[1,2*]

[1]Laboratory of Photobiology, [2]Department of Ophthalmology, [5]Department of Physiology, Keio University School of Medicine, Shinanomachi, Shinjuku-ku, Tokyo, Japan

[3]Department of Life Science and Applied Chemistry, Nagoya Institute of Technology, Nagoya, Aichi, Japan

[4]Section of Viral Vector Development, Center for Genetic Analysis of Behavior, National Institute for Physiological Sciences, National Institutes of Natural Sciences, Okazaki, Aichi, Japan

***Corresponding authors:**

Toshihide Kurihara, MD, PhD

Laboratory of Photobiology, Department of Ophthalmology, Keio University School of Medicine; 35 Shinanomachi, Shinjuku-ku, Tokyo 160-8582, Japan

Tel.: +81-3-5363-3204, Fax: +81-3- 5363-3274

E-mail: kurihara@z8.keio.jp

Kazuo Tsubota, MD, PhD

Professor and Department Chair, Department of Ophthalmology, Keio University School of Medicine; 35 Shinanomachi, Shinjuku-ku, Tokyo 160-8582, Japan

Tel.: +81-3-5363-3269, Fax: +81-3- 3358-5961

E-mail: tsubota@z3.keio.jp

Abstract

Photoreception requires amplification by mammalian rhodopsin through G protein activation, which requires a visual cycle. To achieve this in retinal gene therapy, we incorporated human rhodopsin cytoplasmic loops into *Gloeobacter* rhodopsin, thereby generating *Gloeobacter* and human chimeric rhodopsin (GHCR). In a murine model of inherited retinal degeneration, we induced retinal GHCR expression by intravitreal injection of a recombinant adeno-associated virus vector. Retinal explant and visual thalamus electrophysiological recordings, behavioral tests, and histological analysis showed that GHCR restored dim-environment vision and prevented the progression of retinal degeneration. Thus, GHCR may be a potent clinical tool for the treatment of retinal disorders.

Introduction

Inherited retinal degeneration (IRD) is a major cause of vision loss. More than 2 million people worldwide are blind due to IRD[1], and few effective treatments exist. For retinitis pigmentosa (RP), one of the most common forms of IRD, previous studies have reported vision restoration in animal models using various molecules as optogenetic actuators[2–9]. In addition, clinical trials are under way to investigate the effects of introducing channelrhodopsin 2 (RST-001, ClinicalTrials.gov Identifier: NCT01648452) and ChrimsonR (GS-030, ClinicalTrials.gov Identifier: NCT03326336) into retinal ganglion cells (RGCs) via gene transduction achieved by intravitreal injection of recombinant adeno-associated virus (rAAV). However, microbial opsins, such as channelrhodopsin 2, require high light intensity, such as outdoor light intensity levels, to function[10–12]. They cannot restore vision in dimly lit environments, such as indoors or at night, and strong light irradiation can promote retinal degeneration[13,14]. Physiological photoreception mediated by mammalian rhodopsin, however, relies on amplification through G protein activation. Although the introduction of human rhodopsin improved photosensitivity in mice, it is unclear how the chromophore retinal is metabolized in the retina where the visual cycle is broken. Animal rhodopsin also causes toxicity if all-trans retinal is not properly metabolized[15,16], and is, thus, hampered by safety and stability concerns in terms

54 of clinical application.

55 In this study, to achieve light sensitivity, stability, and safety, we attempted to restore

56 vision in mice using *Gloeobacter* and human chimeric rhodopsin (GHCR)[17,18].

57

58 **Results**

59 **Design of GHCR**

60 Although there is no sequence identity between microbial and animal opsin, both possess

61 similar chromophore (retinal) and protein (seven-transmembrane helix) structures. As we

62 previously reported[18], to generate GHCR, we replaced the second and third intracellular

63 loops of *Gloeobacter* rhodopsin with human sequences and introduced the E132Q

64 mutation (**Figure S1**). Previous work has shown that GHCR induces G protein activation

65 *in vitro*[18].

66

67 **Restoring light-evoked activity in the retina with GHCR**

68 We injected a viral vector (rAAV-DJ or rAAV-2) containing the GHCR coding sequence

69 under the control of the hybrid promoter comprising the CMV immediate-early enhancer,

70 CBA promoter, and CBA intron 1/exon 1, known as the CAGGS promoter,

71 (CAGGS-GHCR; **Figure 1a**) into the vitreous humor of 10-week-old *rd1* mice. We

72 adopted the rAAV-DJ vector to achieve more efficient, widespread gene transfer[19,20], and

73 used rAAV-2 as a benchmark, as it has already been used in the clinic[21]. The retinas were

74 harvested 2–4 months later. Enhanced green fluorescent protein (EGFP) reporter gene

75 expression was observed in the retina and in both the ganglion cell layer and the inner

76 nuclear layer (**Figure S2a, b**). To evaluate the function of ectopically expressed GHCR in

77 the mouse retina, we performed multi-electrode array (MEA) recording to record the

78 extracellular potential of RGCs (**Figure S2c**). As a result of photoreceptor degeneration,

79 the untreated control retina showed no RGC response as detected by MEA (**Figure 1b**). In

80 contrast, the treated retinas showed obvious light-induced responses down to 10^{14}

81 photons/cm^2/s of white light-emitting diode (LED) irradiation (**Figure 1c**).

82 Next, to create a stable vector for human gene therapy, we designed a codon-optimized

83 version of GHCR (coGHCR) and fused the ER2 endoplasmic reticulum (ER) export signal

84 to its C-terminus to increase gene expression levels. Immunolabelling revealed expression

85 across the whole retina, including in the bipolar cells, of treated *rd1* mice (**Figures 1d**). As

86 a result, the firing rate increased significantly, and a photoresponse was confirmed down

87 to 10^{13} photons/cm^2/s, which had not observed before optimization (**Figure 1e, f**).

88 Moreover, the number of firing cells per unit area also increased significantly (**Figure 1g**).

89 Since rhodopsin shows selectivity for Gi/o class G proteins upon heterologous

90 expression[22–25], we measured Gi/o activation with a homogeneous time-resolved
91 fluorescence (HTRF) cyclic adenosine monophosphate (cAMP) assay. We observed a 5-
92 fold increase in activation in coGHCR-treated compared with GHCR-treated mice (**Figure**
93 **1h**). The maximum spectral sensitivity of retinas treated with coGHCR was around 500
94 nm, and a photoresponse was obtained even upon stimulation with light with a wavelength
95 >600 nm (**Figure 1i**).
96
97 **Restoration of visual cortex responses by GHCR**
98 To investigate whether retinal light responses were transmitted to the visual cortex, we
99 then examined visual evoked potentials (VEPs) generated by the visual cortex (**Figure**
100 **2a**). The output from the RGCs is sent through their axons (optic nerve) to the lateral
101 geniculate nucleus (LGN) of the thalamus, which is a region of the diencephalon, then
102 from the LGN to the primary visual cortex in the occipital lobe of the cerebral cortex. For
103 these experiments, we used *rd1* mice in which both eyes had been treated with the AAV-
104 DJ-CAGGS-GHCR, AAV-DJ-CAGGS-coGHCR, or control EGFP (AAV-DJ-CAGGS-
105 EGFP) vectors. Significant VEPs were not detected in the control or GHCR-treated mice.
106 In contrast, VEPs were observed in coGHCR-treated mice (**Figure 2b**). In response to 3
107 cd·s/m^2 light stimulation, the average VEP amplitude in coGHCR-treated mice was

108 significantly higher (56.4 μV; n = 6) than those in GHCR-treated mice (22.1 μV; n = 8)

109 and control mice (17.9 μV; n = 6) (**Figure 2c**). Based on this result, all subsequent

110 experiments were performed using coGHCR.

111

112 **Characterization of the in vivo responses restored by GHCR transduction**

113 Next, light-dark transition (LDT) testing was performed to investigate whether ectopic

114 expression of coGHCR in degenerating retinas led to behavioral changes due to vision

115 restoration (**Figure 3a**). Rodents with intact vision tend to stay in dark places as they are

116 nocturnal and feel uneasy in bright environments, whereas blind rodents spend roughly

117 half of their time in bright places. The coGHCR-treated mice spent significantly less time

118 in the bright area compared with the untreated *rd1* mutant mice (**Figure 3b**), thereby

119 confirming vision restoration via behavioral analysis. Furthermore, in order to directly

120 compare the effects of coGHCR with genes in clinical trials, we treated *rd1* mice with

121 chimeric rhodopsin (AAV-6-CAGGS-coGHCR), microbial opsin (AAV-6-CAGGS-

122 ChrimsonR[26]), animal rhodopsin (AAV-6-CAGGS-human rhodopsin), or the control EGFP

123 (AAV-6-CAGGS-EGFP) vector. At an illuminance of 3,000 lux, a significant reduction in

124 the time spent in the bright half of the observation area was noted for coGHCR-treated

125 mice (0.32; n = 6) compared with control mice (0.50; n = 8) (**Figure 3c**). A similar

126 tendency was observed in ChrimsonR-treated mice (0.36; n = 6). However, no obvious
127 change was observed in human rhodopsin-treated mice (0.48; n = 6). When the experiment
128 was carried out at an illumination of 10 lux, human rhodopsin-treated mice showed a
129 significant change in the time spent in the bright area (0.40; n = 6), whereas ChrimsonR-
130 treated mice did not show an obvious change (0.55; n = 6) (**Figure 3d**). The coGHCR-
131 treated mice again spent significantly less time in the bright area illuminated at 10 lux
132 (0.40; n = 6).
133
134 **Restored object recognition function upon GHCR gene therapy**
135 LDT testing measures only light and dark discrimination. Visual recognition testing
136 (VRT) was performed to evaluate whether the mice could recognize an object with the
137 restored level of vision. Mice use vision for their cognitive functions, and are attracted to
138 fighting videos[27–29]. We examined mice in a place preference apparatus with a tablet
139 showing a fighting video (**Figure 3e**). The ratio of the time spent in the area with the
140 fighting compared with the time spent in the control area (showing a video of an empty
141 cage with the same illuminance) over 15 minutes was measured. The coGHCR-treated
142 (AAV-DJ-CAGGS-coGHCR) mice spent significantly more time in the fighting video half
143 of the apparatus (0.55, n = 33) than the untreated *rd1* mice (0.50, n = 30). On the other

144 hand, microbial opsin-treated (AAV-DJ-CAGGS-C1V1[30]) mice spent roughly equivalent

145 time in each half (0.49, n = 20) (**Figure 3f**).

146

147 **GHCR protective effects against retinal degeneration**

148 We employed another mouse model of retinal degeneration using mice with the P23H

149 *RHO* mutation, referred to as P23H mice[31]. P23H mice were selected to evaluate the

150 protective effect because they have slower retinal degeneration than *rd1* mice. We

151 subretinally delivered AAV DJ-CAGGS-coGHCR and the control (AAV DJ-CAGGS-

152 EGFP) vector into postnatal day (PND) 0–1 mouse retinas, targeting the outer retina, and

153 quantified the protective effects of the vector via morphological and electrophysiological

154 examination. Subretinal injection of AAV-DJ efficiently induced gene expression in the

155 murine outer retina (**Figure 4a**). Optical coherence tomography (OCT) showed that the

156 outer retinal thickness (ORT), which is the thickness from the outer nuclear layer (ONL)

157 to the rod outer segment (ROS), of coGHCR-treated mice (50.0 μm; n = 13) was

158 significantly greater than that of the control mice (42.7 μm; n = 10) at PND 30 (**Figure 4b,**

159 **c**). The ORT of the treated mice remained significantly greater than that of control mice

160 until PND 50 (**Figure S3**).

161 Electroretinography (ERG) revealed that the treated mice had larger rod, mixed, and cone

162 response amplitudes (141.2 μV, 271.4 μV, and 159.0 μV, respectively; n = 9) than the
163 control mice (70.4 μV, 158.7 μV, and 99.1 μV, respectively; n = 14) at PND 30 (**Figure**
164 **4d, e**). All amplitudes in the control mice gradually decreased, whereas all amplitudes in
165 the coGHCR-treated mice continued to increase until PND 42 (**Figure S4a, b c**).
166 Thereafter, the amplitudes in the treated mice also gradually decreased, although they
167 remained significantly higher than those in the control mice until PND 66.
168 We also performed terminal deoxynucleotidyl transferase dUTP nick end labeling
169 (TUNEL) to detect apoptosis in the retinas. The number of TUNEL-positive cells in the
170 coGHCR-treated mouse ONL (289.7 cells; n = 3) was significantly lower than that in the
171 control mouse ONL (67.3 cells; n = 3) at PND 31 (**Figure 5a–c**).
172 To expand these observations, we obtained transmission electron microscopy (TEM)
173 images of transverse sections from PND 31 mice. Consistent with the OCT results, the
174 ONL (**Figure 5d**) and ROS (**Figure 5e**) of coGHCR-treated mice were relatively intact
175 compared with those of controls, and the ROS structure was less disorganized (**Figure 5f**).
176 In addition, coGHCR-treated mice had less swelling of their ER, a feature that is
177 indicative of ER stress (**Figure 5g**).
178 We also performed western blotting to investigate ER stress. Expression of the ER stress
179 marker ATF4 was significantly lower, and expression of BiP, PERK, ATF6, and pIRE1

180 tended to be lower in treated mice than in control mice at PND 14 (**Figure S5a, b**).

181

182 **Discussion**

183 In this study, we demonstrated that ectopic expression of coGHCR is an effective

184 method of vision restoration in mice with retinal degeneration. MEA revealed that

185 photoresponses were maintained for retinal irradiance levels as low as 10^{13} photons/cm^2/s.

186 This is consistent with the response of the treated mice to 10 lux illumination in the

187 behavioral test, and represents a significant improvement in sensitivity compared with that

188 observed in previous studies of vision restoration with microbial opsins (threshold: 10^{14} to

189 10^{17} photons/cm^2/s)[2–7], LiGluR/MAG photoswitches (threshold: 10^{15}–10^{16}

190 photons/cm^2/s)[32,33], or photoactivated ligands (AAQ threshold: 10^{15} photons/cm^2/s[34] and

191 DENAQ threshold: 4×10^{13} photons/cm^2/s[35]). Although some vectors restored greater

192 sensitivity, such as human rhodopsin and Opto-mgluR6 (10^{12} photons/cm^2/s)[8], our LDT

193 results at 3,000 lux (similar to a cloudy outdoor environment) suggest that photobleaching

194 of rhodopsin like these does not work in bright environments. coGHCR is adaptable to a

195 light environment ranging from at least 10 lux (similar to a night light levels with

196 streetlights) to 3,000 lux, and is, thus, a suitable single-opsin vision restoration tool.

197 Furthermore, the typical channelrhodopsins have a spectrum limited to blue light[36],

198 which limits their use as a visual restoration tool. On the other hand, GHCR has a
199 spectrum peak around 500 nm and facilitates responses to red light. In addition, behavioral
200 tests showed that coGHCR enabled responses to both sustained and transient stimulation
201 lasting 10 ms. These findings suggested that coGHCR gene therapy can restore sensitivity
202 to multiple light environments encountered in daily life.

203 The ERG amplitudes in coGHCR-treated mice continued to increase until PND 42, likely
204 because the coGHCR-mediated signal was additive with the innate amplitude. This is
205 consistent with the fact that gene expression of the AAV-DJ vector peaks at approximately
206 1.5 months after administration[19]. We observed no apparent changes in the shapes of the
207 ERG waveforms in the coGHCR-treated mice.

208 coGHCR is known to activate Gt and Gi/o pathways; when expressed ectopically in ON
209 bipolar cells, it is expected to inhibit responses. However, the restored responses observed
210 by MEA were all ON responses. In addition, the electrophysiological and behavioral
211 results were similar to physiological responses, and no reversal reaction observed. In *rd1*
212 mice, photoreceptors are mostly lost by 4 weeks after birth and no optical response is
213 obtained after 7 weeks at the latest[37,38]. Therefore, responses from residual photoreceptors
214 are unlikely in this study. A similar phenomenon has been confirmed in previous studies;
215 the excitatory response is hypothesized to result from disinhibition of inhibitory amacrine

216 cells[6,8,9].

217 The safety of ectopic expression of opsins, such as channelrhodopsin 2, has been

218 previously reported[3,39,40]. To our knowledge, this is the first report of their protective

219 effects against retinal degeneration. In vitro studies have shown that the P23H opsin is

220 misfolded and retained in the ER[41]. ER retention of P23H opsin can induce the unfolded

221 protein response, leading to apoptosis[42–45]. Our results suggest that expression of coGHCR

222 in the retinal outer layer suppressed ER stress and photoreceptor apoptosis, which led to

223 protection against degeneration. The lack of 11-cis-retinal induces cytotoxicity during the

224 development of ROS in P23H mice[46]. Since coGHCR uses all-trans retinal as a

225 chromophore, like microbial opsin, it does not consume cis-retinal and is free from

226 photobleaching. Therefore, the expressed coGHCR may suppress cis-retinal consumption

227 via photoreceptor substitution. If this hypothesis is correct, the protection effect of

228 coGHCR may not be applicable to patients with all IRD genotypes. However, there are

229 more than 140 known RP-linked rhodopsin mutations, and those that result in protein

230 misfolding and retention in the ER are the most prevalent[47,48].

231 In summary, the coGHCR vector has the advantages of both animal and microbial opsin

232 as a vision regeneration tool. It restores sensitivity and an action spectrum that enables

233 vision in lighting ranging from levels found outdoors to those in dimly lit indoor

234 environments via G protein stimulation without the risk of bleaching; it can also be

235 expected to protect against the progression of retinal degeneration in the majority of IRD

236 patients. These results suggest that coGHCR is worthy of consideration for clinical

237 application as a gene therapy for IRD.

238

239 **Methods**

240 Study approval: All of the animal experiments were conducted in accordance with

241 protocols approved by Institutional Animal Care and Use Committee of Keio University

242 School of Medicine (#2808).

243 Please see supplemental information for detail.

Author Contribution

Y.K. and T.K. designed the research, wrote the manuscript. Y.K. performed the retinal histology, MEA, ERG and VEP recordings, and WB, TEM, LDT and VRT experiments. K.Y. performed plasmid construction. K.K. performed AAV production. Y.K. performed data processing and analysis. H.K., H.O and T.K. made critical revisions of the manuscript. T.K. supervised the research.

Acknowledgements

Y.K. was supported by grants from the Keio University Doctorate Student Grant-in-Aid Program and Grant-in-Aid for Research Activity Start-up. T.K. was supported by Grants-in-Aid from Takeda Science Foundation and the Keio University Medical Science Fund. We would like to thank Editage (www.editage.com) for English language editing.

Declaration of Interests

Y.K., H.K., K.T., and T.K. are inventors on pending patents (PCT/JP2017/031579、PCT/JP2019/ 1565) related to this work. Y.K., K.T., and T.K. are equity holders in Restore Vision, Inc.

References

1. Sahel, J.-A., Marazova, K. & Audo, I. Clinical characteristics and current therapies for inherited retinal degenerations. *Cold Spring Harb. Perspect. Med.* **5**, a017111 (2014).
2. Bi, A. *et al.* Ectopic Expression of a Microbial-Type Rhodopsin Restores Visual Responses in Mice with Photoreceptor Degeneration. *Neuron* **50**, 23–33 (2006).
3. Doroudchi, M. M. *et al.* Virally delivered Channelrhodopsin-2 Safely and Effectively Restores Visual Function in Multiple Mouse Models of Blindness. *Mol. Ther.* **19**, 1220–1229 (2011).
4. Lagali, P. S. *et al.* Light-activated channels targeted to ON bipolar cells restore visual function in retinal degeneration. *Nat. Neurosci.* **11**, 667–675 (2008).
5. Cronin, T. *et al.* Efficient transduction and optogenetic stimulation of retinal bipolar cells by a synthetic adeno-associated virus capsid and promoter. *EMBO Mol. Med.* **6**, 1–16 (2014).
6. Macé, E. *et al.* Targeting channelrhodopsin-2 to ON-bipolar cells with vitreally administered AAV restores ON and OFF visual responses in blind mice. *Mol. Ther.* **23**, 7–16 (2014).
7. Busskamp, V. *et al.* Genetic Reactivation of Cone Photoreceptors Restores

Visual Responses in Retinitis Pigmentosa. *Science (80-.).* **329**, 413–417 (2010).

8. Van Wyk, M., Pielecka-Fortuna, J., Löwel, S. & Kleinlogel, S. Restoring the ON Switch in Blind Retinas: Opto-mGluR6, a Next-Generation, Cell- Tailored Optogenetic Tool. *PLoS Biol* **13**, (2015).

9. Pienaar, A., Bedford, R., Davis, K. & Bishop, P. N. Restoration of vision with ectopic expression of human rod opsin. *Curr. Biol.* **25**, 1–35 (2015).

10. Kleinlogel, S. *et al.* Ultra light-sensitive and fast neuronal activation with the Ca 2+-permeable channelrhodopsin CatCh. *Nat. Neurosci.* **14**, 513–518 (2011).

11. Kleinlogel, S. *et al.* A gene-fusion strategy for stoichiometric and co-localized expression of light-gated membrane proteins. *Nat. Methods* **8**, 1083–1091 (2011).

12. Pan, Z. H., Ganjawala, T. H., Lu, Q., Ivanova, E. & Zhang, Z. ChR2 mutants at L132 and T159 with improved operational light sensitivity for vision restoration. *PLoS One* **9**, (2014).

13. Grimm, C. *et al.* Protection of Rpe65-deficient mice identifies rhodopsin as a mediator of light-induced retinal degeneration. *Nat. Genet.* **25**, 63–66 (2000).

14. Vaughan, D. K., Coulibaly, S. F., Darrow, R. M. & Organisciak, D. T. A morphometric study of light-induced damage in transgenic rat models of retinitis pigmentosa. *Investig. Ophthalmol. Vis. Sci.* **44**, 848–855 (2003).

15. Różanowska, M. & Sarna, T. Light-induced Damage to the Retina: Role of Rhodopsin Chromophore Revisited. *Photochem. Photobiol.* **81**, 1305 (2005).

16. Maeda, A. *et al.* Involvement of all-trans-retinal in acute light-induced retinopathy of mice. *J. Biol. Chem.* **284**, 15173–15183 (2009).

17. Nakatsuma, A. *et al.* Chimeric microbial rhodopsins containing the third cytoplasmic loop of bovine rhodopsin. *Biophys. J.* **100**, 1874–1882 (2011).

18. Sasaki, K. *et al.* Chimeric Proton-Pumping Rhodopsins Containing the Cytoplasmic Loop of Bovine Rhodopsin. *PLoS One* **9**, e91323 (2014).

19. Katada, Y., Kobayashi, K., Tsubota, K. & Kurihara, T. Evaluation of AAV-DJ vector for retinal gene therapy. *PeerJ*

20. Grimm, D. *et al.* In vitro and in vivo gene therapy vector evolution via multispecies interbreeding and retargeting of adeno-associated viruses. *J. Virol.* **82**, 5887–5911 (2008).

21. Keeler, A. M. & Flotte, T. R. Recombinant Adeno-Associated Virus Gene Therapy in Light of Luxturna (and Zolgensma and Glybera): Where Are We, and How Did We Get Here? *Annu. Rev. Virol.* **6**, 601–621 (2019).

22. Bailes, H. J. & Lucas, R. J. Human melanopsin forms a pigment maximally sensitive to blue light (λmax ≈ 479 nm) supporting activation of Gq/11 and Gi/o

signalling cascades. *Proc. R. Soc. B Biol. Sci.* **280**, (2013).

23. Li, X. *et al.* Fast noninvasive activation and inhibition of neural and network activity by vertebrate rhodopsin and green algae channelrhodopsin. *Proc. Natl. Acad. Sci. U. S. A.* **102**, 17816–17821 (2005).

24. Gutierrez, D. V. *et al.* Optogenetic control of motor coordination by G i/o protein-coupled vertebrate rhodopsin in cerebellar purkinje cells. *J. Biol. Chem.* **286**, 25848–25858 (2011).

25. Cao, P. *et al.* Light-sensitive coupling of rhodopsin and melanopsin to G i/o and G q signal transduction in Caenorhabditis elegans . *FASEB J.* **26**, 480–491 (2012).

26. Klapoetke, N. C. *et al.* Independent optical excitation of distinct neural populations. *Nat. Methods* **11**, 338–346 (2014).

27. Watanabe, S., Shinozuka, K. & Kikusui, T. Preference for and discrimination of videos of conspecific social behavior in mice. *Anim. Cogn.* **19**, 523–531 (2016).

28. Watanabe, S. Preference for and Discrimination of Paintings by Mice. *PLoS One* **8**, (2013).

29. Yakura, T. *et al.* Visual recognition of mirror, video-recorded, and still images in rats. *PLoS One* **13**, 1–11 (2018).

30. Erbguth, K., Prigge, M., Schneider, F., Hegemann, P. & Gottschalk, A. Bimodal Activation of Different Neuron Classes with the Spectrally Red-Shifted Channelrhodopsin Chimera C1V1 in Caenorhabditis elegans. *PLoS One* **7**, (2012).

31. Sakami, S., Kolesnikov, A. V., Kefalov, V. J. & Palczewski, K. P23H opsin knock-in mice reveal a novel step in retinal rod disc morphogenesis. *Hum. Mol. Genet.* **23**, 1723–1741 (2014).

32. Caporale, N. *et al.* LiGluR restores visual responses in rodent models of inherited blindness. *Mol. Ther.* **19**, 1212–1219 (2011).

33. Gaub, B. M. *et al.* Restoration of visual function by expression of a light-gated mammalian ion channel in retinal ganglion cells or ON-bipolar cells. (2014). doi:10.1073/pnas.1414162111

34. Polosukhina, A. *et al.* Photochemical Restoration of Visual Responses in Blind Mice. *Neuron* **75**, 271–282 (2012).

35. Tochitsky, I. *et al.* Restoring visual function to blind mice with a photoswitch that exploits electrophysiological remodeling of retinal ganglion cells. *Neuron* **81**, 800–813 (2014).

36. Nagel, G. *et al.* Channelrhodopsin-2, a directly light-gated cation-selective

membrane channel. *Proc. Natl. Acad. Sci. U. S. A.* **100**, 13940–5 (2003).

37. Fujii, M., Sunagawa, G. A., Kondo, M., Takahashi, M. & Mandai, M. Evaluation of micro Electroretinograms Recorded with Multiple Electrode Array to Assess Focal Retinal Function. *Sci. Rep.* 1–12 (2016). doi:10.1038/srep30719

38. Chang, B. *et al.* Two mouse retinal degenerations caused by missense mutations in the beta-subunit of rod cGMP phosphodiesterase gene. *Vision Res.* **47**, 624–33 (2007).

39. Sugano, E. *et al.* Immune responses to adeno-associated virus type 2 encoding channelrhodopsin-2 in a genetically blind rat model for gene therapy. *Gene Ther.* **18**, 266–274 (2011).

40. Ivanova, E. & Pan, Z. H. Evaluation of the adeno-associated virus mediated long-term expression of channelrhodopsin-2 in the mouse retina. *Mol. Vis.* **15**, 1680–1689 (2009).

41. Chapple, J. P. *et al.* Unfolding retinal dystrophies: A role for molecular chaperones? *Trends Mol. Med.* **7**, 414–421 (2001).

42. Liu, X., Garriga, P. & Khorana, H. G. Structure and function in rhodopsin: Correct folding and misfolding in two point mutants in the intradiscal domain of rhodopsin identified in retinitis pigmentosa. *Proc. Natl. Acad. Sci. U. S. A.* **93**,

4554–4559 (1996).

43. Frederick, J. M. *et al.* Mutant rhodopsin transgene expression on a null background. *Investig. Ophthalmol. Vis. Sci.* **42**, 826–833 (2001).

44. Leonard, K. C. *et al.* XIAP protection of photoreceptors in animal models of retinitis pigmentosa. *PLoS One* **2**, (2007).

45. Lin, J. H. *et al.* IRE1 signaling affects cell fate during the unfolded protein response. *Science (80-.).* **318**, 944–949 (2007).

46. Sakami, S. *et al.* Probing mechanisms of photoreceptor degeneration in a new mouse model of the common form of autosomal dominant retinitis pigmentosa due to P23H opsin mutations. *J. Biol. Chem.* **286**, 10551–10567 (2011).

47. Mendes, H. F., Van Der Spuy, J., Chapple, J. P. & Cheetham, M. E. Mechanisms of cell death in rhodopsin retinitis pigmentosa: Implications for therapy. *Trends Mol. Med.* **11**, 177–185 (2005).

48. Yoshida, T. *et al.* The use of induced pluripotent stem cells to reveal pathogenic gene mutations and explore treatments for retinitis pigmentosa. *Mol. Brain* **7**, 1–11 (2014).

Figure legends

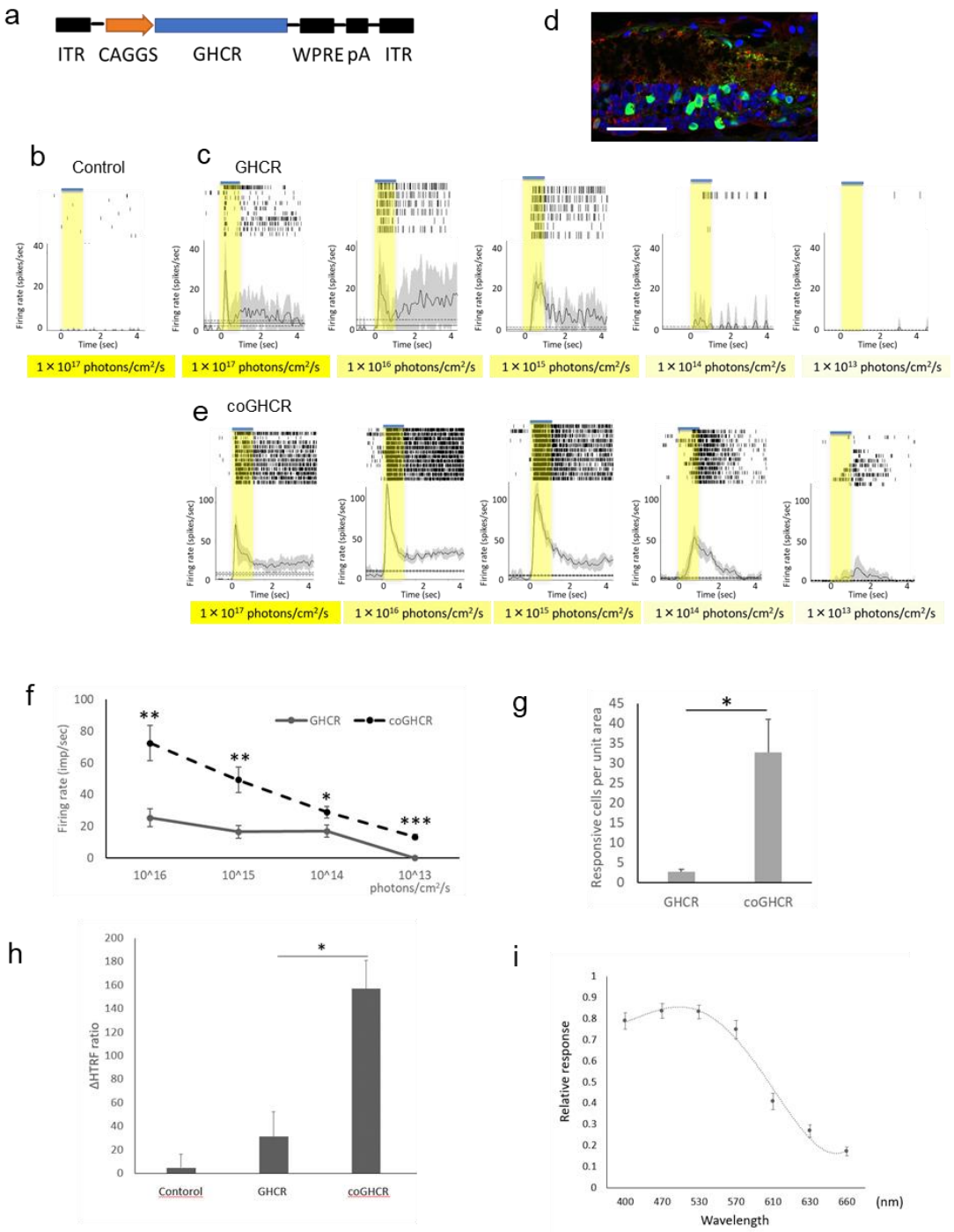

Figure 1. Ectopic GHCR expression restores light responses in the *rd1* mouse retina

(a) DNA expression cassette schematic. The GHCR coding sequence is driven by the CAGGS promoter, flanked by inverted terminal repeats (ITR), and stabilized by a polyadenylation signal sequence (pA) and a woodchuck hepatitis posttranscriptional regulatory element (WPRE). (b, c, e) Raster plots and peri-stimulus time histograms for light stimulation of control (AAV-DJ-CAGGS-EGFP) (b), GHCR-treated (AAV-DJ-CAGGS-GHCR) (c), and coGHCR-treated (AAV-DJ-CAGGS-coGHCR) mice (e). Responses to exposure to a white LED with varying light intensity for 1.0 s. Gray shading around the averaged traces represents the standard error of the mean (SEM). (d) Confocal image of a transverse *rd1* mouse retina section 2 months after AAV-DJ-CAGGS-coGHCR intravitreal injection. Green, FLAG tag antibody signal (vector); red, PKCα signal (bipolar cells); blue, 4′,6-diamidino-2-phenylindolenuclear (DAPI) counterstaining. Scale bar, 50 μm. (f) Quantitation of the firing rates of RGCs transduced with GHCR or coGHCR at the indicated light intensity. (g) Histogram showing the number of RGCs that responded to light per unit area (2.6 mm^2) of the retinas of GHCR- or coGHCR-treated mice (n = 3 each). (g) Changes in cAMP consumption in response to Gi/o-coupled G-

protein-coupled receptor activation in HEK293T cells transfected with GHCR and coGHCR (n = 3 each). (h) Spectral sensitivity induced by coGHCR. Error bars represent the SEM. Data were analyzed with Student's two-tailed t-test; * represents $p < 0.05$, ** represents $p < 0.01$, and *** represents $p < 0.001$.

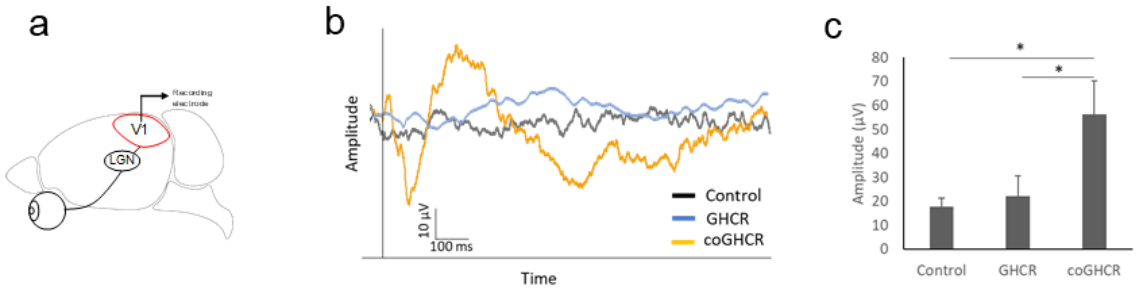

Figure 2. coGHCR restored vision in *rd1* mice through the primary visual cortex

(a) Schematic view of the VEP recording strategy. (b) Representative VEP traces from GHCR-treated, coGHCR-treated, and control mice. (c) The average amplitude of the VEPs in the control (AAV-DJ-CAGGS-EGFP), GHCR-treated (AAV-DJ-CAGGS-GHCR), and coGHCR-treated (AAV-DJ-CAGGS-coGHCR) mice. The stimulus was a white LED flash (3 cd·s/m^2). Signals were low-pass filtered at 300 Hz and averaged over 60 trials. Error bars represent the SEM. Data were analyzed with one-way analysis of variance (ANOVA) and Tukey's multiple comparison test; * represents $p < 0.05$. V1, visual cortex.

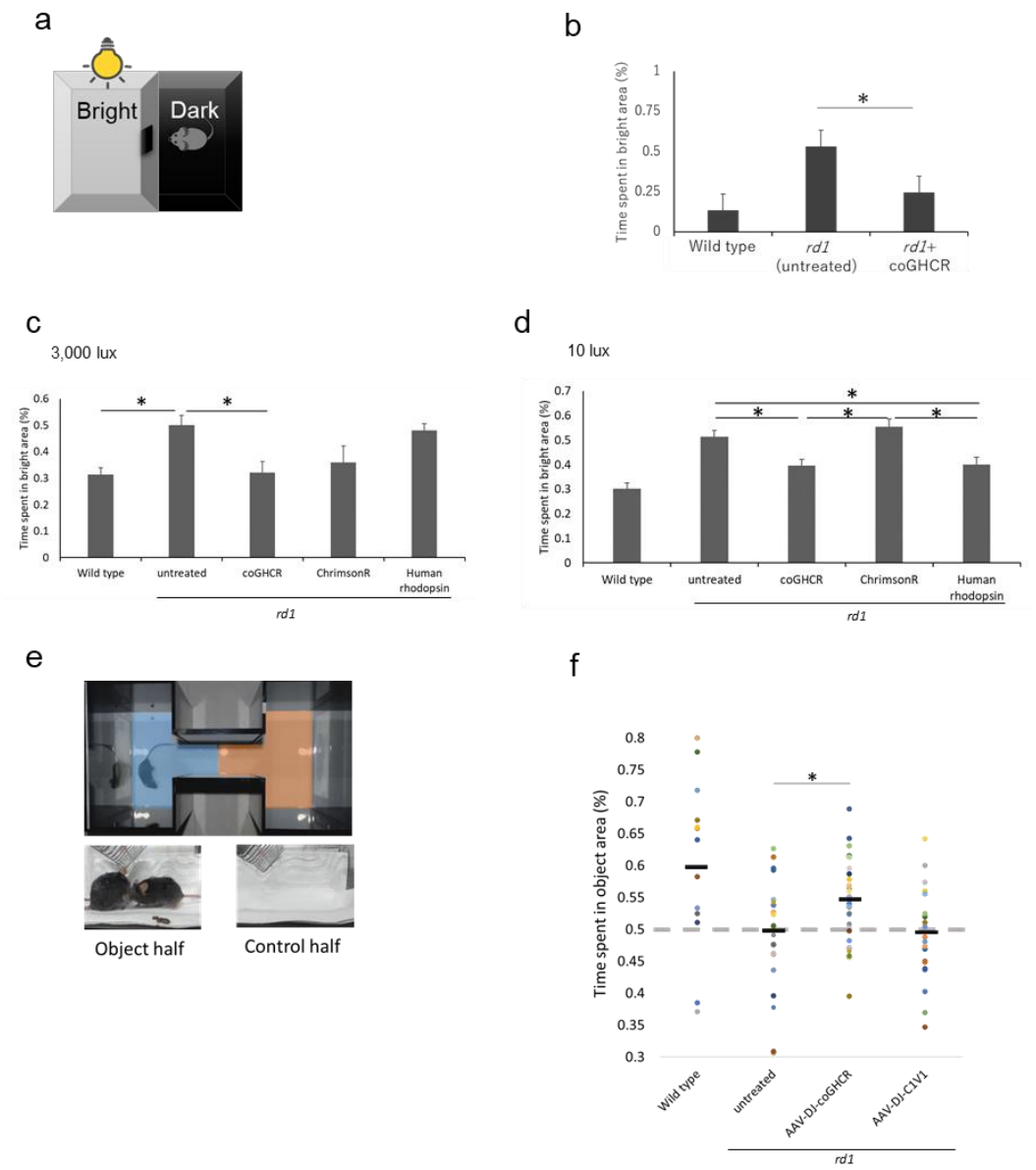

Figure 3. coGHCR-treated mouse behavior indicated vision restoration

(a) LDT testing schematic. Mice were tested in a 30 × 45 × 30-cm box with equally sized bright and dark chambers connected by a 5 × 5-cm opening, across which the mice could move freely. (b) Percentage of time spent in the bright area (total, 10 min) by wild type (n

= 4), and control (AAV-DJ-CAGGS-EGFP) (n = 7) and coGHCR-treated (AAV-DJ-CAGGS-coGHCR) *rd1* mice (n = 6). LDT test, 10 lux illumination. (c, d) The percentage of time spent in the bright area (total, 10 min) by wild type (n = 6), and control (AAV-6-CAGGS-EGFP) (n = 8), coGHCR-treated (AAV-6-CAGGS-coGHCR) (n = 6), ChrimsonR-treated (AAV-6-CAGGS-ChrimsonR) (n = 6), and human rhodopsin-treated (AAV-6-CAGGS-human-rhodopsin) *rd1* mice (n = 6). LDT test with 3,000 lux (c) and 10 lux (d) illumination. (e) VRT setup. Time spent in areas showing a video of mice fighting (object half, blue) or an empty cage (control half, red) was measured. (f) Distribution of time spent in the object half by wild type (n = 6), and control (no treatment) (n = 8), AAV-2-coGHCR-treated (AAV-2-CAGGS-coGHCR) (n = 6), AAV-DJ-coGHCR-treated (AAV-DJ-CAGGS- coGHCR) (n = 6), and AAV-DJ-C1V1-treated (AAV-DJ-CAGGS-C1V1) *rd1* mice (n = 6). LDT test with 10 lux (c) and 3,000 lux (d) illumination. Black line, average value. Error bars represent the SEM. Data were analyzed with one-way ANOVA and Tukey's multiple comparison test; * represents $p < 0.05$, ** represents $p < 0.01$, and *** represents $p < 0.001$.

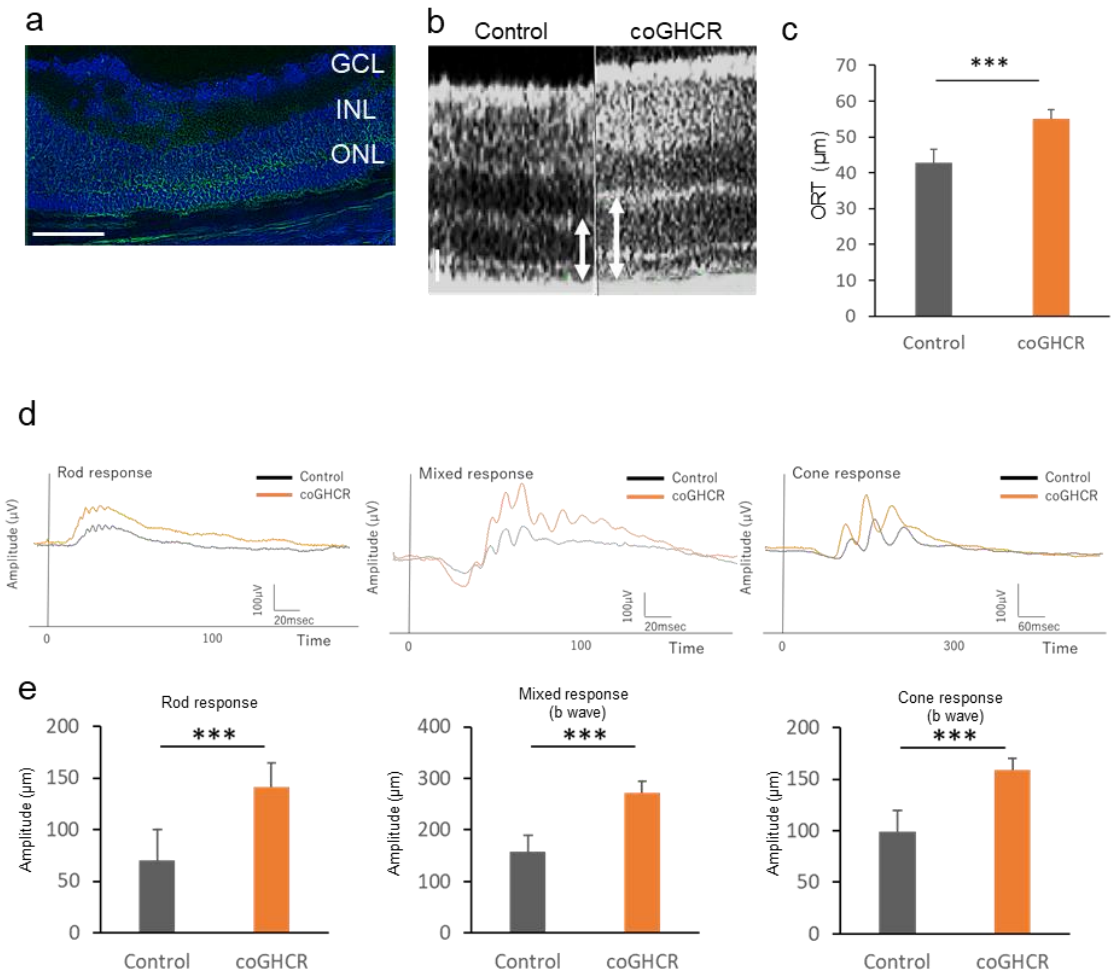

Figure 4. Ectopic coGHCR expression protects against photoreceptor degeneration

(a) Confocal image of a transverse section through the P23H retina 2 months after AAV-DJ-CAGGS-coGHCR subretinal injection. Green, FLAG tag fused to the C-terminus of coGHCR; blue, DAPI nuclear counterstaining. Scale bar, 100 μm. (b) OCT retinal image sections from coGHCR-treated and control (AAV-DJ-CAGGS-EGFP subretinally injected) mice at PND 30. The white arrow indicates the measured ORT (from ONL to cone outer segment). Scale bar, 20 μm. (c) Histogram of the measured ORT of the

coGHCR-treated and control mice at PND 30. (d, e) Representative ERG waveforms (rod response, mixed response, and cone response) of coGHCR-treated and control mice (d). Histograms of the average ERG amplitudes from panel d at PND 30 (e). Error bars represent SEM. Data were analyzed with the unpaired t-test; *** represents $p < 0.001$. GCL, ganglion cell layer; INL, inner nuclear layer.

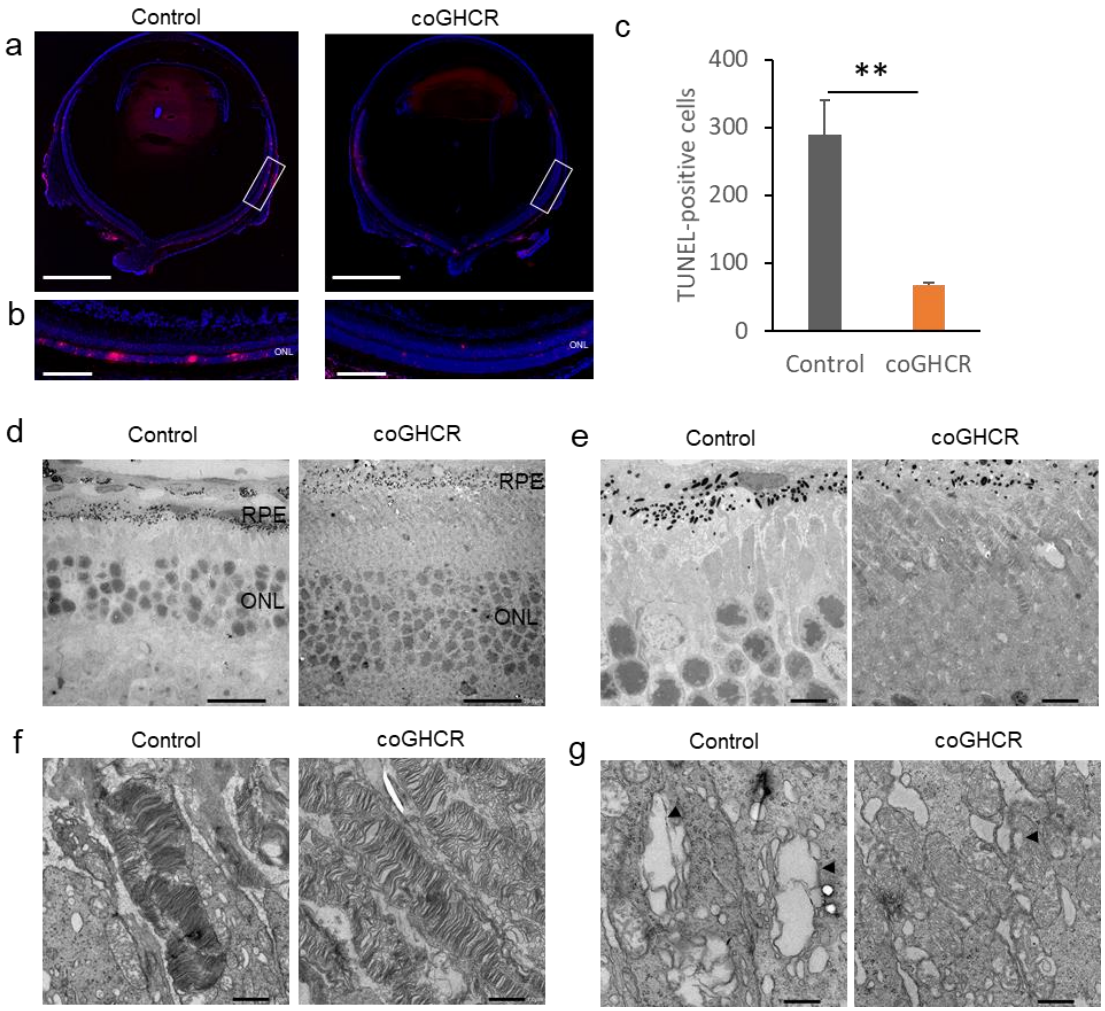

Figure 5. coGHCR treatment suppressed retinal apoptosis and ER stress

(a, b) TUNEL-stained transverse sections (a) and enlarged images of the white squares (b) of coGHCR-treated and control (AAV-DJ-CAGGS-EGFP subretinally injected) mouse retinas at PND 31. Red, TUNEL-positive cells; blue, DAPI nuclear counterstaining. Scale bar, 1,000 μm in (a) and 100 μm in (b). (c) Histogram of the number of TUNEL-positive cells in the ONLs of coGHCR-treated and control mice at PND 31. Error bars represent SEM. Data were analyzed with the unpaired t-test; ** represents $p < 0.01$. (d) TEM images of transverse sections from coGHCR-treated and control mice at PND 31, showing the outer retinal layer (d), the outer segment at low magnification (e) and high magnification (f), and the inner segment (g). The arrowhead indicates swollen ER. Scale bar, 20 μm in (d), 5 μm in (e), 1 μm in (f), and 500 nm in (g).